Current Biology 22, 70–77, January 10, 2012 ©2012 Elsevier Ltd All rights reserved DOI 10.1016/j.cub.2011.11.043

Report

A Role for the Melatonin-Related Receptor GPR50 in Leptin Signaling, Adaptive Thermogenesis, and Torpor

David A. Bechtold,[1,*] Anissa Sidibe,[2,3,4] Ben R.C. Saer,[1] Jian Li,[1] Laura E. Hand,[1] Elena A. Ivanova,[1] Veerle M. Darras,[5] Julie Dam,[2,3,4] Ralf Jockers,[2,3,4] Simon M. Luckman,[1] and Andrew S.I. Loudon[1,*]
[1]Faculty of Life Sciences, University of Manchester, Manchester M13 9PT, UK
[2]Inserm, U1016, Institut Cochin, Paris, France
[3]CNRS UMR 8104, Paris, France
[4]Université Paris Descartes, Sorbonne Paris Cite, 75006 Paris, France
[5]Laboratory of Comparative Endocrinology, Katholieke Universiteit Leuven, 3000 Leuven, Belgium

Summary

The ability of mammals to maintain a constant body temperature has proven to be a profound evolutionary advantage, allowing members of this class to thrive in most environments on earth. Intriguingly, some mammals employ bouts of deep hypothermia (torpor) to cope with reduced food supply and harsh climates [1, 2]. During torpor, physiological processes such as respiration, cardiac function, and metabolic rate are severely depressed, yet the neural mechanisms that regulate torpor remain unclear [3]. Hypothalamic responses to energy signals, such as leptin, influence the expression of torpor [4–7]. We show that the orphan receptor GPR50 plays an important role in adaptive thermogenesis and torpor. Unlike wild-type mice, *Gpr50*$^{-/-}$ mice readily enter torpor in response to fasting and 2-deoxyglucose administration. Decreased thermogenesis in *Gpr50*$^{-/-}$ mice is not due to a deficit in brown adipose tissue, the principal site of nonshivering thermogenesis in mice [8]. GPR50 is highly expressed in the hypothalamus of several species, including man [9, 10]. In line with this, altered thermoregulation in *Gpr50*$^{-/-}$ mice is associated with attenuated responses to leptin and a suppression of thyrotropin-releasing hormone. Thus, our findings identify hypothalamic circuits involved in torpor and reveal GPR50 to be a novel component of adaptive thermogenesis in mammals.

Results and Discussion

Severe Hypometabolism in *Gpr50*$^{-/-}$ Mice upon Fasting

We demonstrated previously that in comparison to wild-type (WT) littermates, *Gpr50*$^{-/-}$ mice show resistance to diet-induced obesity, yet lose less weight when fasted [9]. Intense GPR50 immunoreactivity (IR) is observed in the neurons of the dorsomedial nucleus (DMN) of the hypothalamus and tanycytes that line the third ventricle (Figures 1A–1D; see also Figure S1 available online), both implicated in nutrient sensing and energy balance [11, 12]. This prompted us to further characterize the metabolic phenotype of the *Gpr50*$^{-/-}$ mice. Long-term recording of body temperature (T_b) revealed *Gpr50*$^{-/-}$ mice to have a lower nighttime T_b compared with WT mice, despite showing 25% higher locomotor activity (Figures 1E and 1F). Remarkably, upon fasting, *Gpr50*$^{-/-}$ mice consistently entered a state of torpor, characterized by severe drops in metabolic rate (VO_2) (Figures 1G and 1I) and T_b (25.8°C±0.7; Figures 1H and 1I). The depth of hypothermia was not dependent on ambient temperatures (T_a) of 23°C or 16°C (Figure 1; Figure S2). The temporal profile of torpor indicated that the process was gated by the circadian clock; this was confirmed by housing mice under constant light (removing exogenous timing cues) and fasting for 48 hr (Figure 1J). Two distinct torpor bouts with defined circadian profiles were observed in the *Gpr50*$^{-/-}$ mice. Torpor was not observed in WT mice during 48 hr of food deprivation, demonstrating that torpor is not driven simply by depletion of energy stores. Further, the expression of torpor in knockout (KO) mice was not due to inherent differences in body weight between the genotypes (Figure S2C). Torpor has been reported previously in laboratory mice. However, profound hypothermia (<30°C) has typically been observed only following prolonged food restriction and reduced T_a [7, 13–16]. *Gpr50*$^{-/-}$ mice enter a state of torpor (T_b ~25°C) within as little as 6 hr of fasting when housed at constant T_a of ~23°C, which is characterized by a stable level of hypothermia.

In line with reduced T_b, expression of uncoupling protein 1 (*ucp1*) in brown adipose tissue (BAT) was lower in *Gpr50*$^{-/-}$ mice than WT animals (Figure 1K). Nonetheless, KO mice exhibited a normal elevation in T_b and BAT expression of *ucp1* and deiodinase 2 (*dio2*) in response to the β_3-adrenergic receptor agonist CL-316243 (Figures 1L and 1M; Figure S2D). The robust response of the *Gpr50*$^{-/-}$ mice to β_3-adrenergic receptor stimulation demonstrates that the low nocturnal T_b and expression of torpor in these mice are not due to diminished thermogenic capacity or responsiveness of BAT, but rather likely reflect altered sympathetic drive to this tissue. It is also possible that heat loss may be accentuated in the *Gpr50*$^{-/-}$ mice, for example through alterations in sympathetic control of blood flow.

Fasted *Gpr50*$^{-/-}$ mice exhibited significantly lower circulating glucose in comparison with WT mice (*Gpr50*$^{-/-}$, 3.9 mmol/l ± 0.4; WT, 5.4 ± 0.3; $p < 0.05$) suggesting that hypoglycemia could contribute to the torpor response. Consistent with this, *Gpr50*$^{-/-}$ mice were found to be hypersensitive to deoxyglucose (2-DG), a glucose mimetic that induces a state of perceived hypoglycemia. KO mice exhibited torpor-like drops in VO_2 and T_b following doses of 2-DG (250–500 mg/kg) that had little effect on WT mice (Figure S3). However, both genotypes exhibited comparable rises in blood glucose in response to 2-DG (Figure S3), indicating that the exaggerated metabolic response of the *Gpr50*$^{-/-}$ mice is not due to diminished glucose storage or ineffective counter-regulatory glucose release. Similarly, no genotype differences in glucose clearance were observed during a glucose tolerance test ($p > 0.05$, two-way analysis of variance; Figure S3E). Tanycytes express much of the glucose-sensing machinery employed by pancreatic β-cells [17], and selective destruction of these cells attenuates 2-DG-induced feeding in rats [18]. This suggests

*Correspondence: david.bechtold@manchester.ac.uk (D.A.B.), andrew.loudon@manchester.ac.uk (A.S.I.L.)

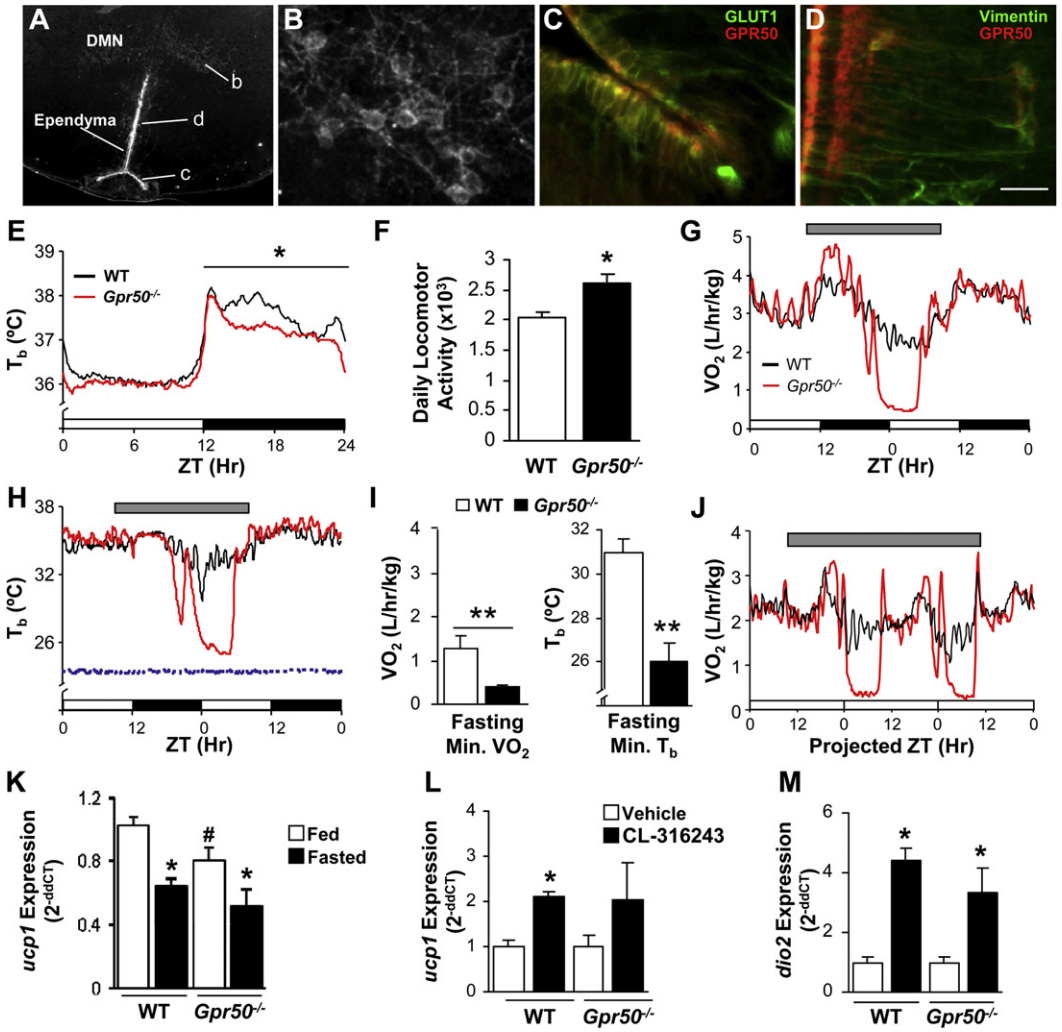

Figure 1. Altered Thermogenesis in *Gpr50*$^{-/-}$ Mice

(A–D) GPR50 immunoreactivity in the brain is limited to the ventral portion of the third ventricle ependymal layer (A) and neurons of the DMN.

(B–D) The identity of GPR50 expressing cells as tanycytes was confirmed by colocalization of the receptor (red) with the tanycyte markers GLUT1 (C; green) and vimentin (D; green). Lowercase letters in (A) represent the approximate positions of (B), (C), and (D). Nonmerged images are available in Figure S1. GPR50 expression was undetectable in *Gpr50* knockout (KO) mice used in the current studies (Figure S1). Scale bar represents 200 μm in (A) and 15 μm in (B–D).

(E and F) Mean body temperature (T_b) and locomotor activity in wild-type (WT) and *Gpr50*$^{-/-}$ mice collected over 30 days of monitoring (n = 8/group). Nighttime T_b was reduced in *Gpr50*$^{-/-}$ mice (E), despite a 25% increase in locomotor activity (F).

(G–J) Representative recordings of O_2 consumption (VO_2; G) and T_b (H) records in *Gpr50*$^{-/-}$ and WT mice subjected to a 24 hr fast in which *Gpr50*$^{-/-}$ mice entered a state of torpor (n = 8–10/group, group data shown in I). Fasting period is represented by the gray bar above trace, and ambient room temperature is represented by the hashed line in (H). The following abbreviation is used: ZT, zeitgeber time (ZT0 indicates lights on).

(J) To remove exogenous timing cues, we housed mice in constant light and fasted for 48 hr (n = 4/group). *Gpr50*$^{-/-}$ mice exhibited two distinct and precisely timed torpor bouts.

(K) Lower *ucp1* expression was observed in brown adipose tissue (BAT) from *Gpr50*$^{-/-}$ mice compared with WT mice in either a fed or fasted state (n = 6–12/group).

(L and M) Administration of the β_3-adrenergic receptor agonist CL-316243 (1 mg/kg intraperitoneal [ip]) elicited comparable increases in *ucp1* (L) and *dio2* (M) expression in BAT in WT and *Gpr50*$^{-/-}$ mice. Thermogenic responses to CL-316243 are shown in Figure S2.

(E–M) Data is shown as mean ± SE with *$p < 0.05$ and **$p < 0.01$ Student's t test (E–I); *$p < 0.05$ versus fed or vehicle and #$p < 0.05$ versus WT using a two-way analysis of variance (ANOVA) and Bonferonni's post hoc test (K–M).

that GPR50 signaling in tanycytes modulates the response of these cells to changes in glucose.

Altered Hypothalamic Thyroid Hormones Are Not Sufficient to Drive Torpor

Tanycytes play a central role in dictating T_3 availability within the hypothalamus [19–21], and local T_3 signaling is implicated in hypothalamic responses to fasting [20]. Extensive colocalization of GPR50 (red) and the T_3-transporter MCT8 (green) was observed in tanycytes (Figure 2A). Expression of *mct8* was significantly induced in the ependymal layer and paraventricular nucleus (PVN) of WT mice in response to fasting (Figures 2C and 2D). This induction was observed in the PVN, but not the ependymal layer of *Gpr50*$^{-/-}$ mice (Figures 2F and 2G). The T_3-converting enzyme *dio2* was also strongly induced in the ependymal layer of fasted WT mice (Figures 2B

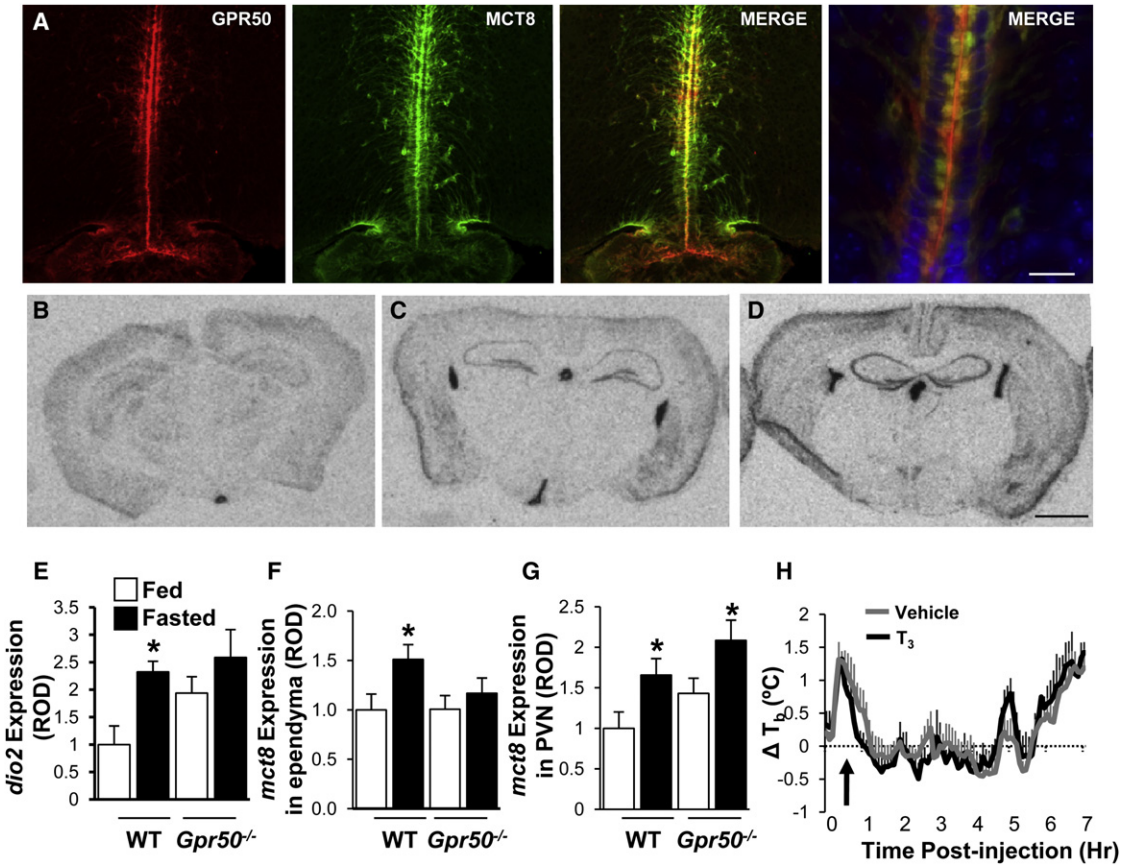

Figure 2. Loss of *Gpr50* Alters Thyroid Hormone Availability in the Hypothalamus

(A) Extensive colocalization of GPR50 (red) and MCT8 (green) was observed in tanycyte cell bodies and processes. Blue represents DAPI staining. Scale bar represents 100 μm in the three left panels and 10 μm in the right panel.

(B–F) Hypothalamic expressions of *dio2* and *mct8* and were determined by in situ hybridization in fed and fasted WT and $Gpr50^{-/-}$ mice (n = 6–8/group). Autoradiographs are representative of *dio2* (B) and *mct8* (C and D) expression, in fasted WT (B and C) or $Gpr50^{-/-}$ (D) mice. Fasting induced the expression of *dio2* (E) and *mct8* (F) in the ependymal layer of WT mice. Constitutive expression of *dio2* was elevated in the knockouts. Fasting also led to a significant increase in *mct8* expression in the paraventricular nucleus (PVN) of WT and $Gpr50^{-/-}$ mice. Increased *dio2* expression was reflected in hypothalamic T_3 in $Gpr50^{-/-}$ mice ($Gpr50^{-/-}$, 3.9 ± 0.3 pmol/g; WT, 3.3 ± 0.2).

(G) Data is shown as mean ± SE with *p < 0.05 versus fed and #p < 0.05 versus WT using two-way ANOVA and Bonferonni's post hoc test. Scale bar represents 1.6 mm in (B)–(D).

(H) Central administration of T_3 had no acute effects on T_b in WT mice (8 ng, intracerebroventricular [icv], n = 5/group).

and 2E). Interestingly, *dio2* expression was constitutively elevated in fed $Gpr50^{-/-}$ mice, achieving a similar level as that of fasted WT mice. These findings demonstrate that GPR50 modulates T_3 handling in tanycytes and that altered T_3 availability may therefore influence thermogenesis. A role for hypothalamic T_3 in seasonal torpor has been suggested [22]. However, neither acute (Figure 2H) nor chronic (Figure S3) administration of T_3 altered T_b in WT mice, suggesting that changes in T_3 are not sufficient to drive torpor and that a secondary signal of reduced energy status must be required.

GPR50 Modulates Leptin Signaling In Vivo and In Vitro

Leptin is a peripherally derived indicator of energy status that acts at multiple sites within the hypothalamus, including the DMN [23, 24]. Leptin is capable of blocking torpor in seasonal species [4–6], and mice deficient in leptin (*ob/ob*) are prone to torpor despite their massive fat reserves [5, 7]. Interestingly, *Gpr50* expression in the DMN is significantly reduced in *ob/ob* mice but can be increased to levels seen in control mice (*ob/wt*) by leptin treatment (Figures 3A–3D). Both GPR50 and leptin receptor (Ob-Rb; LepR) are expressed at high levels in the DMN (Figure 3E; [24]). Thus, attenuated *Gpr50* expression may facilitate torpor in *ob/ob* mice, and the induction of GPR50 may be an underlying mechanism by which leptin blocks torpor in *ob/ob* mice and other species [4, 5]. Leptin-responsive *Gpr50* expression was confirmed in vitro, where leptin administration to *Ob-Rb*-expressing cells significantly enhanced *Gpr50* promoter-driven luciferase activity (Figure 3F; Figure S4).

To test the ability of leptin to block torpor in $Gpr50^{-/-}$ mice, we treated fasted WT and KO mice with leptin 2 to 3 hr prior to the onset of torpor. Leptin administration blocked fasting-induced drops in VO_2 in WT mice (Figures 3G–3I; Figure S4). In contrast, central or peripheral administration of leptin was unable to attenuate torpor in the $Gpr50^{-/-}$ mice, despite the ability of leptin to block torpor in other mouse and hamster models [5, 25]. Furthermore, in comparison to WT mice, leptin-induced thermogenesis was also attenuated in KO mice in a fed state (Figures 3J and 3K; Figure S4). The reduced efficacy of leptin on $Gpr50^{-/-}$ mice was specific to thermogenesis,

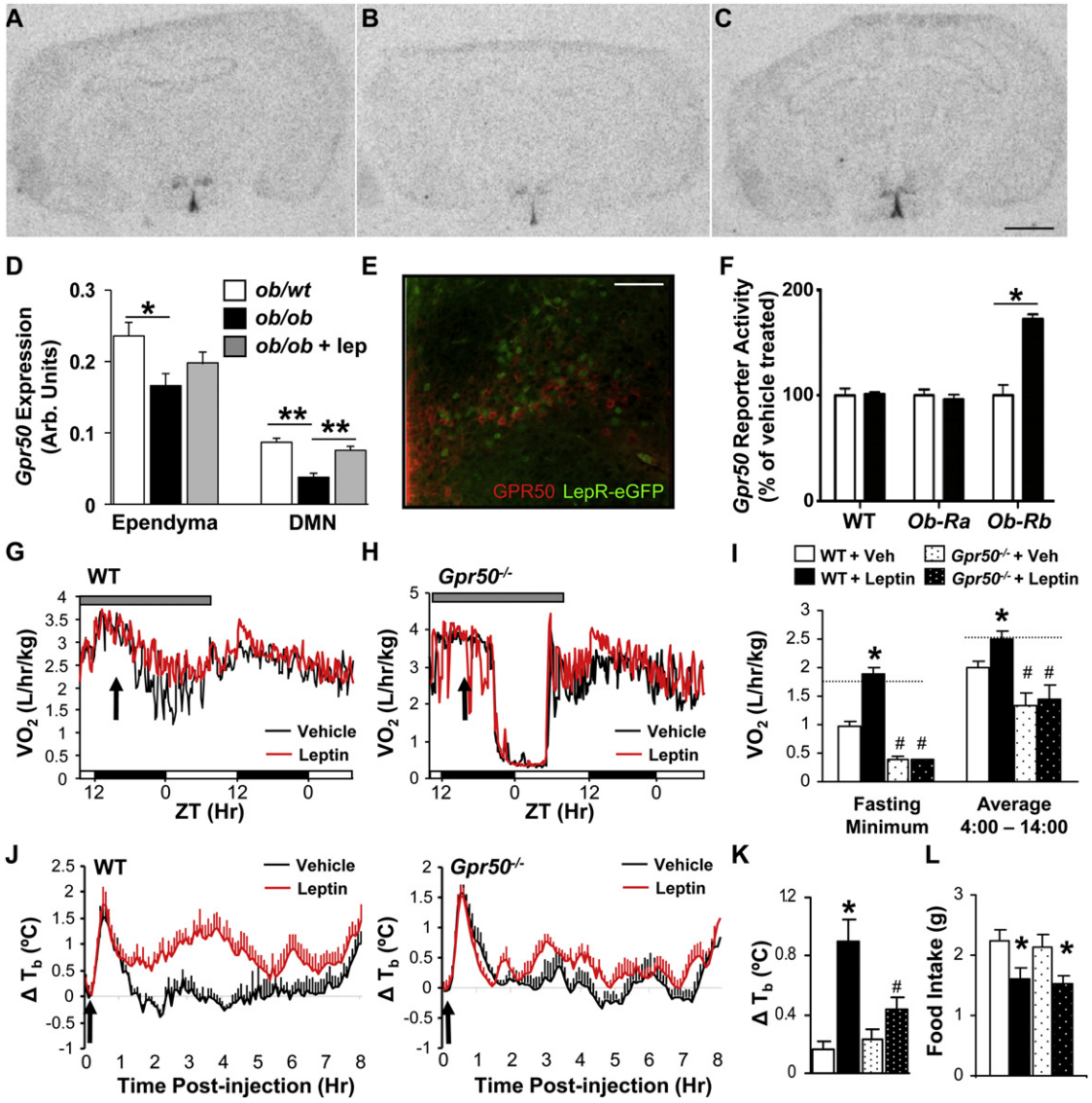

Figure 3. Interaction of GPR50 and Leptin

(A–D) *Gpr50* expression in torpor-prone *ob/ob* mice was examined by in situ hybridization (n = 8/group). In comparison with control *ob/wt* mice (A), *Gpr50* expression was lower in *ob/ob* mice (B) in both the DMN and the ependymal layer of the third ventricle (D). *Gpr50* expression could be rescued by administration of exogenous leptin (2 mg/kg/day, ip) for 5 days (C and D). Data is shown as mean ± SE with *p < 0.05 and **p < 0.01 using a one-way ANOVA and Bonferonni's post hoc test. Scale bar represents 1.5 mm.

(E) Dual immunolocalization of GPR50 (red) and LepR-eGFP (green) in the DMN. Scale bar represents 80 μm.

(F) Leptin-responsive *Gpr50* promoter activity. Leptin (100 nM) elicited a significant increase in *Gpr50*-luciferase reporter activity in HEK293 cells stably expressing *OB-Rb*, but not in WT or *OB-Ra*-expressing cells. Induction of *Gpr50* by leptin was also dependent on Jak2 and PI3K (Figure S4). Results are normalized first to an internal renilla-luciferase control, then to the activity of vehicle treated cells. No alteration in *Gpr50* reporter activity was observed following leptin treatment of cells expressing the short (nonsignaling) form of the leptin receptor (*Ob-Ra*). Data is shown as mean ± SE with *p < 0.05 versus control using a Student's t test.

(G–I) Administration of leptin at midnight (ZT17) prevented the fasting-induced drop in metabolic rate in WT mice (G), yet did not alter the expression or depth of torpor in the *Gpr50*$^{-/-}$ mice (H; 200 pmol, icv, n = 6/group). Dashed lines in (I) reflect VO_2 recorded the previous day during ad libitum feeding.

(J and K) Leptin administration to fed WT mice increased T_b for approximately 6 hr (J; n = 6–8/group). The thermogenic response to leptin was significantly attenuated in *Gpr50*$^{-/-}$ mice (J and K).

(L) To assess the effects of leptin on feeding, we administered leptin at the onset of the dark phase of the light cycle and ad libitum nocturnal food intake monitored (200 pmol, icv, n = 8/group). The anorexic actions of leptin were maintained in *Gpr50*$^{-/-}$ mice. Data is shown as mean ± SE with *p < 0.05 versus vehicle and #p < 0.05 versus WT using a two-way ANOVA and Bonferonni's post hoc test.

because leptin administration remained equally effective at reducing nocturnal food intake in both genotypes (Figure 3L). These results demonstrate that the feeding-related and thermogenic actions of leptin can be clearly differentiated and that only the latter is modulated by GPR50. A similar segregation of the anorexic and thermogenic actions of leptin has been demonstrated in mice in which melanocortin signaling has been targeted [26–28]. Specifically, loss of the MCR4 receptor blocks the effects of leptin on sympathetic outflow to BAT, adipose gene expression, and fat mass,

Table 1. Impact of GPR50 on Transcriptional Response to Leptin

Condition			Increased expression	Decreased expression	Total
Ob-Rb	vs	*Ob-Rb* + Gpr50	299	307	606
Ob-Rb	vs	*Ob-Rb* + Leptin	827	490	1,327
Ob-Rb	vs	*Ob-Rb* + Gpr50 + leptin	1,605	1,100	2,705
Ob-Rb + leptin	vs	*Ob-Rb* + Gpr50 + leptin	1,022	1,016	2,038

$p < 0.05$ considered a change in gene expression. Functional pathway analysis revealed that genes exhibiting a significant change in expression, following leptin administration when cells express both *Ob-Rb* and *Gpr50*, are implicated in range of cellular processes, including amino acid transport, lipid metabolism, and metabolic disease (Figure S5).

whereas the anorexic actions of leptin are maintained [27, 28]. The ability of GPR50 to influence cellular responses to leptin was assessed in vitro by gene microarray. This study revealed that the proportion of genes showing a significant alteration in expression following leptin treatment was substantially higher (2,705 genes) in cells expressing *Ob-Rb* in combination with *Gpr50*, compared with cells expressing *Ob-Rb* alone (1,327 genes) (Table 1; Figure S5).

Our work reveals a critical role for GPR50 in leptin signaling. We show that *Gpr50* expression is both responsive to leptin and essential for the full impact of leptin signaling on energy expenditure in vivo.

Depressed Expression of Hypothalamic TRH Underlies Altered Thermogenesis

GPR50 exhibits an intense and restricted expression pattern within the hypothalamus, a structure that is a major regulator of BAT activity. Within the hypothalamus, the involvement of arcuate nucleus (ARC) neurons in fasting and leptin responsive thermoregulation is well established [29], and the ARC projects heavily to both the PVN and DMN. Further, neuropeptide Y (NPY) and melanocortin signaling have been directly implicated in torpor [30, 31], and administration of the melanocortin receptor agonist MTII elevates BAT thermogenesis and T_b [32]. Yet surprisingly, *Gpr50*$^{-/-}$ and WT mice exhibit a similar expression of ARC neuropeptides *npy*, *agrp*, *pomc*, and *cart* (Figure S4). Further, administration of MTII did not dampen torpor in the *Gpr50*$^{-/-}$ mice (Figures 4A–4C), despite blocking torpor in other models [31]. Metabolic rate was increased by MTII in fed *Gpr50*$^{-/-}$ mice (Figure S4), demonstrating that the mice are not deficient in melanocortin sensitivity per se but that GPR50 modulates its impact during fasting.

ARC neurons project heavily to corticotropin-releasing hormone (CRH) and thyrotropin-releasing hormone (TRH)-expressing neurons of the PVN both directly and via the DMN [33, 34]. These populations are important in regulating energy balance and drive neuroendocrine and autonomic outputs of the hypothalamus. Quantification of *CRH* and *TRH* expression revealed clear differences between WT and *Gpr50*$^{-/-}$ mice (Figures 4D and 4E). In contrast to WT mice, fasting did not elicit a rise in *CRH* expression in the PVN of *Gpr50*$^{-/-}$ mice. Constitutive expression of *TRH* was also significantly lower in *Gpr50*$^{-/-}$ mice compared with WT mice. Fasting further inhibited *TRH* expression in both genotypes. *TRH* was also significantly reduced in the anterior hypothalamus of KO mice when compared with WT mice (Figure S3), but transcriptional changes were not universal, because *CRH* expression in the amygdala and *TRH* expression in the DMN did not differ significantly between genotypes. Central TRH administration increases BAT activity [35, 36], suggesting that depressed expression of *TRH* in the PVN and AH of *Gpr50*$^{-/-}$ mice underpins their hypometabolic phenotype. Central administration of RX77368 (a stable analog of TRH) blocked torpor in *Gpr50*$^{-/-}$ mice (Figures 4F–4H) indicating that attenuated *TRH* is indeed a causal mechanism in the thermogenic responses of the *Gpr50*$^{-/-}$ mice.

GPR50, Ob-Rb, and MCR4 receptors are all highly expressed in the DMN (here and [37–40]), suggesting that loss of GPR50 in the DMN contributes to decreased thermogenesis under normal and fasted conditions, as well as the attenuated response to leptin and MTII. That we did not observe any differences in the expression of *npy*, *agrp*, *pomc*, or *cart* within the ARC of WT and *Gpr50*$^{-/-}$ mice is in accord with a central role for the DMN in altered thermogenic response of the KO mice. We envision that GPR50 neurons in the DMN modulate thermogenesis via brainstem sites that innervate BAT [41–43] and/or by modulating *TRH*-expressing neurons in the hypothalamus. The absence of GPR50-IR in the PVN (Figure S1) necessitates that the influence of GPR50 on *TRH* expression in the PVN is indirect; the most likely route being via DMN neurons known to contact CRH and TRH neurons in the PVN [34]. Through this pathway, GPR50 would serve to modulate DMN relay of fasting- and leptin-related signals to other hypothalamic and brainstem nuclei.

Conclusions

In seasonal species, rhythmic torpor bouts are not controlled by proximal changes in food supply but require long-term metabolic adaption, which accompanies seasonal changes in daylength (photoperiod). Physiological responses to photoperiod cycles are driven by melatonin. Our studies now reveal that GPR50, an ortholog of the avian melatonin Mel1C receptor [44], has evolved a new role: as a critical modulator of adaptive thermogenesis and torpor. That we have now linked reduced expression of *Gpr50* with heightened torpor response in three models, Siberian hamsters [45], leptin deficient (*ob/ob*) mice, and *Gpr50* knockout mice, implies that GPR50 normally serves to repress entry into a hypometabolic state by modulating thermal responses to energy signals such as glucose and leptin.

Experimental Procedures

Animals and Surgical Procedures

Gpr50$^{-/-}$ mice were generated by DeltaGen (CA, USA) and obtained via AstraZeneca (Alderley Park, Cheshire, UK) [9]. *Ob/ob* mice were purchased from Charles River (UK). Age-matched or littermate male mice were used in all experiments and maintained under a 12-12 hr light-dark schedule, unless stated otherwise. Studies were licensed under the Animals Act of 1986 and local animal welfare committee. Implantation of intracerebroventricular (icv) guide cannulae and remote telemetry probes (DataScience International, The Netherlands) was as previously described [46].

Indirect Calorimetry, 2-DG, and Blood Glucose

Metabolic gases (O_2 and CO_2) were measured using indirect calorimetric cages (Columbus Instruments, Columbus, OH, USA). Icv injection of mouse leptin (200 pmol; Sigma), RX77368 (2 ng, gift from Professors Geoffrey Bennett and Fran Ebling, University of Nottingham), T_3 (8 ng, Sigma) or

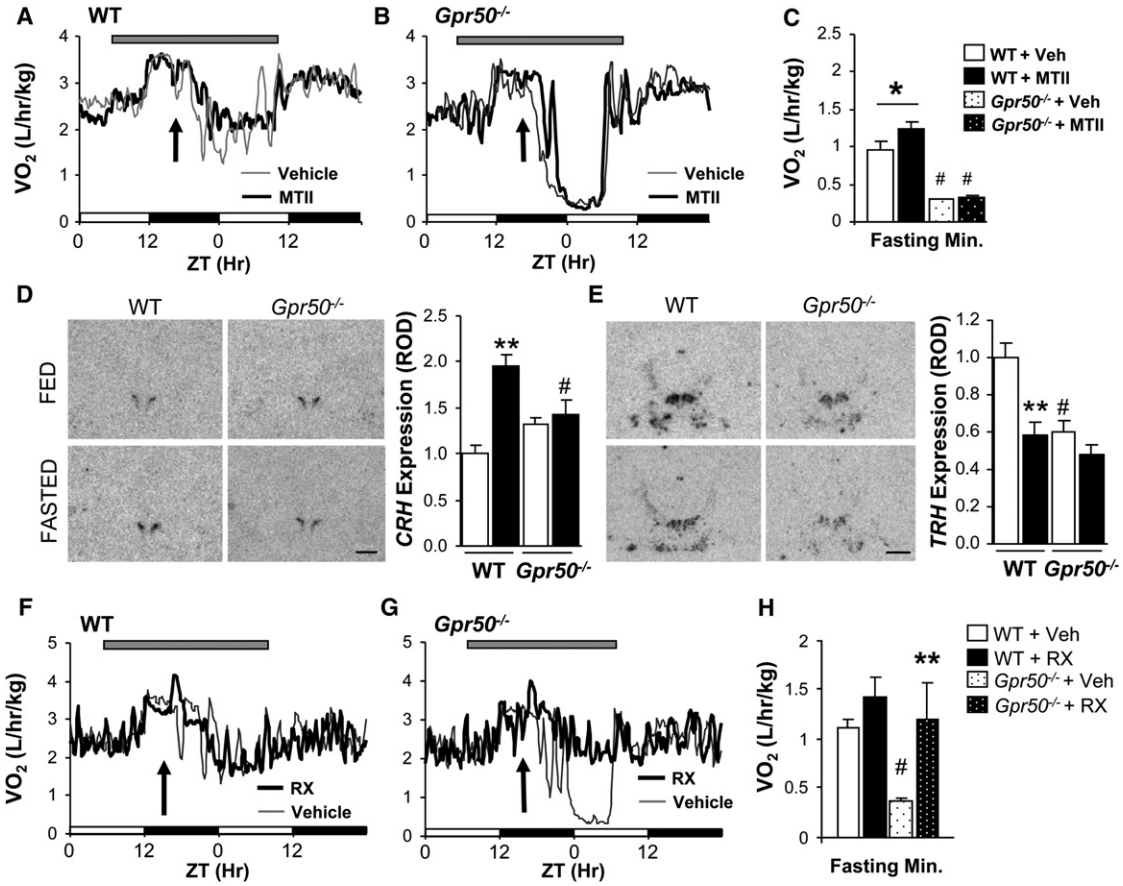

Figure 4. Association of Torpor with Depressed TRH Expression in the Hypothalamus

(A–C) Administration of MTII at midnight (ZT17) increased metabolic rate in fasted WT mice (A and C) but did not alter the expression or depth of torpor in the *Gpr50*$^{-/-}$ mice (B and C; 1 nmol, icv, n = 4–6/group). Data is shown as mean ± SE with *p < 0.05 versus vehicle and #p < 0.05 versus WT using a two-way ANOVA and Bonferonni's post hoc test.

(D and E) Expression of *CRH* (D) and thyrotropin releasing hormone (*TRH*) (E) were quantified in the PVN of WT and *Gpr50*$^{-/-}$ mice under fed (top) and fasted (bottom) conditions by in situ hybridization histology (n = 8/group). WT mice exhibited a significant induction of *CRH* expression in response to fasting, whereas no such change was observed in *Gpr50*$^{-/-}$ mice (D). A significant decrease in *TRH* expression was observed in the PVN of WT mice upon fasting (E). *TRH* expression in ad libitum fed *Gpr50*$^{-/-}$ mice was significantly lower than that of WT mice and was reduced further upon fasting (F). Data is shown as mean ± SE with **p < 0.01 versus fed and #p < 0.05 versus WT using a two-way ANOVA and Bonferonni's post hoc test. Scale bar represents 800 μm.

(F–H) Central administration of the TRH agonist RX77368 (2 μg, icv) to fasted WT (n = 4/group; F) and *Gpr50*$^{-/-}$ mice (n = 8/group; G) prevented the fasting-induced drop in VO_2 in *Gpr50*$^{-/-}$ mice (H). Data is shown as mean ± SE with **p < 0.01 versus vehicle and #p < 0.05 versus WT using a two-way ANOVA and Bonferonni's post hoc test.

vehicle (0.9% NaCl) were delivered in 1 μl over a period of 30 s. During 2-DG (Sigma) administration, food was removed and circulating glucose measured by tail tip bleed with an Optimum Plus glucose meter (Abbott Laboratories, UK). Mice were acclimated to calorimetric cages, handling, and blood collection for 2 days prior to study.

In Situ Hybridization and Real-Time Quantitative PCR

Tissues were processed as previously described [1, 47]. Primers used for generating riboprobes (in situ) and qPCR probes are listed in the Supplemental Information. TRH, CRH, and Dio2 probes were kindly provided by Dr. Perry Barrett (University of Aberdeen, UK). Products were cloned into p-GEMT Easy Vector (Promega, Madison, USA), riboprobes synthesized with ^{33}P-UTP (MP Biomedical, USA), and hybridization visualized by film autoradiography (Kodak BioMax MR film, Kodak, USA). Optical density was determined using 3–4 sections/mouse/area. QPCR was performed using the Platinum SyBR Green Kit (Invitrogen). Housekeeping genes *18S* rRNA or cyclophilin were used as controls.

Immunohistochemistry

Brains were removed and fixed for 48 hr in Bouin's fixative (Sigma). Frozen sections (20–30 μm) were blocked with serum followed by primary and secondary antibodies (see Supplemental Experimental Procedures). Omission of primary or secondary antibody resulted in no positive immunoreaction.

Reporter Gene Activation Assay

HEK293 stable cell lines expressing human *OB-Rb* or *OB-Ra* were cotransfected with a *Gpr50* luciferase reporter plasmid (257 bp upstream of *Gpr50* start codon; 250 ng) and a Renilla luciferase plasmid (25 ng). Cells were then treated with or without leptin (100 nM) for 6 hr after 1 hr pretreatment with or without 50 μM AG490 or 50 μM Wortmanin (Sigma). Luciferase activity was normalized to renilla activity.

μ-Array Experiments

HEK293 cells stably expressing *OB-Rb* were transfected with a *Gpr50* expression plasmid or mock transfected and treated with or without leptin (100 nM) for 6 hr. RNA was purified and validated (using Agilent RNA6000 nano chip kit; Bioanalyzer 2100). Complementary DNA was produced, end labeled with biotin, hybridized to GeneChip® human Gene (Affymetrix), and scanned using the GCS3000 7G. Images were analyzed with Expression Console software (Affymetrix). Robust multichip average (RMA) was normalized using the RMA option of Expression Console and subjected to statistical analysis. Pathway analysis was performed with the Ingenuity program.

Supplemental Information

Supplemental Information includes five figures and Supplemental Experimental Procedures and can be found with this article online at doi:10.1016/j.cub.2011.11.043.

Acknowledgments

We thank John Brennand (AstraZeneca, UK) for providing *Gpr50*$^{-/-}$ mice, Thomas Bourgeron (Institut Pasteur, Paris) for kindly providing the *Gpr50*-luc reporter, and Martin Myers Jr. (University of Michigan) for kindly providing *LepR*-eGFP tissue. Microarray experiments and data analysis were performed by the Genomic Facility of the Cochin Institute. This work was supported by grants from the Biotechnology and Biological Sciences Research Council (S.M.L., A.S.I.L.), Equipe Fondation Recherche Médicale (J.D., R.J.), Institut National de la Santé et de la Recherche Médicale (J.D., R.J.), and Centre National de la Recherche Scientifique (J.D., R.J.).

Received: July 18, 2011
Revised: November 3, 2011
Accepted: November 21, 2011
Published online: December 22, 2011

References

1. Heldmaier, G., Ortmann, S., and Elvert, R. (2004). Natural hypometabolism during hibernation and daily torpor in mammals. Respir. Physiol. Neurobiol. *141*, 317–329.
2. Geiser, F. (2004). Metabolic rate and body temperature reduction during hibernation and daily torpor. Annu. Rev. Physiol. *66*, 239–274.
3. Melvin, R.G., and Andrews, M.T. (2009). Torpor induction in mammals: recent discoveries fueling new ideas. Trends Endocrinol. Metab. *20*, 490–498.
4. Webb, G.P., Jagot, S.A., and Jakobson, M.E. (1982). Fasting-induced torpor in Mus musculus and its implications in the use of murine models for human obesity studies. Comp. Biochem. Physiol. Comp. Physiol. *72*, 211–219.
5. Gavrilova, O., Leon, L.R., Marcus-Samuels, B., Mason, M.M., Castle, A.L., Refetoff, S., Vinson, C., and Reitman, M.L. (1999). Torpor in mice is induced by both leptin-dependent and -independent mechanisms. Proc. Natl. Acad. Sci. USA *96*, 14623–14628.
6. Freeman, D.A., Lewis, D.A., Kauffman, A.S., Blum, R.M., and Dark, J. (2004). Reduced leptin concentrations are permissive for display of torpor in Siberian hamsters. Am. J. Physiol. Regul. Integr. Comp. Physiol. *287*, R97–R103.
7. Gluck, E.F., Stephens, N., and Swoap, S.J. (2006). Peripheral ghrelin deepens torpor bouts in mice through the arcuate nucleus neuropeptide Y signaling pathway. Am. J. Physiol. Regul. Integr. Comp. Physiol. *291*, R1303–R1309.
8. Cannon, B., and Nedergaard, J. (2004). Brown adipose tissue: function and physiological significance. Physiol. Rev. *84*, 277–359.
9. Ivanova, E.A., Bechtold, D.A., Dupré, S.M., Brennand, J., Barrett, P., Luckman, S.M., and Loudon, A.S. (2008). Altered metabolism in the melatonin-related receptor (GPR50) knockout mouse. Am. J. Physiol. Endocrinol. Metab. *294*, E176–E182.
10. Sidibe, A., Mullier, A., Chen, P., Baroncini, M., Boutin, J.A., Delagrange, P., Prevot, V., and Jockers, R. (2010). Expression of the orphan GPR50 protein in rodent and human dorsomedial hypothalamus, tanycytes and median eminence. J. Pineal Res. *48*, 263–269.
11. Nilaweera, K., Herwig, A., Bolborea, M., Campbell, G., Mayer, C.D., Morgan, P.J., Ebling, F.J., and Barrett, P. (2011). Photoperiodic regulation of glycogen metabolism, glycolysis, and glutamine synthesis in tanycytes of the Siberian hamster suggests novel roles of tanycytes in hypothalamic function. Glia *59*, 1695–1705.
12. Dimicco, J.A., and Zaretsky, D.V. (2007). The dorsomedial hypothalamus: a new player in thermoregulation. Am. J. Physiol. Regul. Integr. Comp. Physiol. *292*, R47–R63.
13. Tsukada, M., Hamade, N., Wada, Y., Mogi, T., Kamiyama, S., and Koizumi, A. (1993). Energy restriction suppresses microsomal Ca(2+)-ATPase activities in various organs in C57BL/6 female mice in both euthermic and torpor states. Mech. Ageing Dev. *68*, 183–189.
14. Rikke, B.A., Yerg, J.E., 3rd, Battaglia, M.E., Nagy, T.R., Allison, D.B., and Johnson, T.E. (2003). Strain variation in the response of body temperature to dietary restriction. Mech. Ageing Dev. *124*, 663–678.
15. Zhang, J., Kaasik, K., Blackburn, M.R., and Lee, C.C. (2006). Constant darkness is a circadian metabolic signal in mammals. Nature *439*, 340–343.
16. Swoap, S.J., Gutilla, M.J., Liles, L.C., Smith, R.O., and Weinshenker, D. (2006). The full expression of fasting-induced torpor requires beta 3-adrenergic receptor signaling. J. Neurosci. *26*, 241–245.
17. García, M.A., Millán, C., Balmaceda-Aguilera, C., Castro, T., Pastor, P., Montecinos, H., Reinicke, K., Zúñiga, F., Vera, J.C., Oñate, S.A., and Nualart, F. (2003). Hypothalamic ependymal-glial cells express the glucose transporter GLUT2, a protein involved in glucose sensing. J. Neurochem. *86*, 709–724.
18. Sanders, N.M., Dunn-Meynell, A.A., and Levin, B.E. (2004). Third ventricular alloxan reversibly impairs glucose counterregulatory responses. Diabetes *53*, 1230–1236.
19. Rodríguez, E.M., Blázquez, J.L., Pastor, F.E., Peláez, B., Peña, P., Peruzzo, B., and Amat, P. (2005). Hypothalamic tanycytes: a key component of brain-endocrine interaction. Int. Rev. Cytol. *247*, 89–164.
20. Coppola, A., Liu, Z.W., Andrews, Z.B., Paradis, E., Roy, M.C., Friedman, J.M., Ricquier, D., Richard, D., Horvath, T.L., Gao, X.B., and Diano, S. (2007). A central thermogenic-like mechanism in feeding regulation: an interplay between arcuate nucleus T3 and UCP2. Cell Metab. *5*, 21–33.
21. López, M., Varela, L., Vázquez, M.J., Rodríguez-Cuenca, S., González, C.R., Velagapudi, V.R., Morgan, D.A., Schoenmakers, E., Agassandian, K., Lage, R., et al. (2010). Hypothalamic AMPK and fatty acid metabolism mediate thyroid regulation of energy balance. Nat. Med. *16*, 1001–1008.
22. Murphy, M., Jethwa, P.H., Warner, A., Barrett, P., Nilaweera, K.N., Brameld, J.M., and Ebling, F.J. (2011). Effects of Manipulating Hypothalamic Triiodothyronine Concentrations on Seasonal Body Weight and Torpor Cycles in Siberian Hamsters. Endocrinology, in press. Published online October 25, 2011.
23. Gautron, L., Lazarus, M., Scott, M.M., Saper, C.B., and Elmquist, J.K. (2010). Identifying the efferent projections of leptin-responsive neurons in the dorsomedial hypothalamus using a novel conditional tracing approach. J. Comp. Neurol. *518*, 2090–2108.
24. Patterson, C.M., Leshan, R.L., Jones, J.C., and Myers, M.G., Jr. (2011). Molecular mapping of mouse brain regions innervated by leptin receptor-expressing cells. Brain Res. *1378*, 18–28.
25. Döring, H., Schwarzer, K., Nuesslein-Hildesheim, B., and Schmidt, I. (1998). Leptin selectively increases energy expenditure of food-restricted lean mice. Int. J. Obes. Relat. Metab. Disord. *22*, 83–88.
26. Satoh, N., Ogawa, Y., Katsuura, G., Numata, Y., Masuzaki, H., Yoshimasa, Y., and Nakao, K. (1998). Satiety effect and sympathetic activation of leptin are mediated by hypothalamic melanocortin system. Neurosci. Lett. *249*, 107–110.
27. Ste Marie, L., Miura, G.I., Marsh, D.J., Yagaloff, K., and Palmiter, R.D. (2000). A metabolic defect promotes obesity in mice lacking melanocortin-4 receptors. Proc. Natl. Acad. Sci. USA *97*, 12339–12344.
28. Zhang, Y., Kilroy, G.E., Henagan, T.M., Prpic-Uhing, V., Richards, W.G., Bannon, A.W., Mynatt, R.L., and Gettys, T.W. (2005). Targeted deletion of melanocortin receptor subtypes 3 and 4, but not CART, alters nutrient partitioning and compromises behavioral and metabolic responses to leptin. FASEB J. *19*, 1482–1491.
29. Elmquist, J.K., Coppari, R., Balthasar, N., Ichinose, M., and Lowell, B.B. (2005). Identifying hypothalamic pathways controlling food intake, body weight, and glucose homeostasis. J. Comp. Neurol. *493*, 63–71.
30. Dark, J., and Pelz, K.M. (2008). NPY Y1 receptor antagonist prevents NPY-induced torpor-like hypothermia in cold-acclimated Siberian hamsters. Am. J. Physiol. Regul. Integr. Comp. Physiol. *294*, R236–R245.
31. Mounien, L., Marty, N., Tarussio, D., Metref, S., Genoux, D., Preitner, F., Foretz, M., and Thorens, B. (2010). Glut2-dependent glucose-sensing controls thermoregulation by enhancing the leptin sensitivity of NPY and POMC neurons. FASEB J. *24*, 1747–1758.
32. Brito, M.N., Brito, N.A., Baro, D.J., Song, C.K., and Bartness, T.J. (2007). Differential activation of the sympathetic innervation of adipose tissues by melanocortin receptor stimulation. Endocrinology *148*, 5339–5347.
33. Cone, R.D. (2005). Anatomy and regulation of the central melanocortin system. Nat. Neurosci. *8*, 571–578.
34. Lechan, R.M., and Fekete, C. (2006). The TRH neuron: a hypothalamic integrator of energy metabolism. Prog. Brain Res. *153*, 209–235.

35. Griffiths, E.C., Rothwell, N.J., and Stock, M.J. (1988). Thermogenic effects of thyrotrophin-releasing hormone and its analogues in the rat. Experientia *44*, 40–42.
36. Rogers, R.C., Barnes, M.J., and Hermann, G.E. (2009). Leptin "gates" thermogenic action of thyrotropin-releasing hormone in the hindbrain. Brain Res. *1295*, 135–141.
37. Elmquist, J.K., Ahima, R.S., Elias, C.F., Flier, J.S., and Saper, C.B. (1998). Leptin activates distinct projections from the dorsomedial and ventromedial hypothalamic nuclei. Proc. Natl. Acad. Sci. USA *95*, 741–746.
38. Kishi, T., Aschkenasi, C.J., Lee, C.E., Mountjoy, K.G., Saper, C.B., and Elmquist, J.K. (2003). Expression of melanocortin 4 receptor mRNA in the central nervous system of the rat. J. Comp. Neurol. *457*, 213–235.
39. Bi, S., Robinson, B.M., and Moran, T.H. (2003). Acute food deprivation and chronic food restriction differentially affect hypothalamic NPY mRNA expression. Am. J. Physiol. Regul. Integr. Comp. Physiol. *285*, R1030–R1036.
40. Caron, E., Sachot, C., Prevot, V., and Bouret, S.G. (2010). Distribution of leptin-sensitive cells in the postnatal and adult mouse brain. J. Comp. Neurol. *518*, 459–476.
41. Cano, G., Passerin, A.M., Schiltz, J.C., Card, J.P., Morrison, S.F., and Sved, A.F. (2003). Anatomical substrates for the central control of sympathetic outflow to interscapular adipose tissue during cold exposure. J. Comp. Neurol. *460*, 303–326.
42. Oldfield, B.J., Giles, M.E., Watson, A., Anderson, C., Colvill, L.M., and McKinley, M.J. (2002). The neurochemical characterisation of hypothalamic pathways projecting polysynaptically to brown adipose tissue in the rat. Neuroscience *110*, 515–526.
43. Morrison, S.F. (2004). Activation of 5-HT1A receptors in raphe pallidus inhibits leptin-evoked increases in brown adipose tissue thermogenesis. Am. J. Physiol. Regul. Integr. Comp. Physiol. *286*, R832–R837.
44. Dufourny, L., Levasseur, A., Migaud, M., Callebaut, I., Pontarotti, P., Malpaux, B., and Monget, P. (2008). GPR50 is the mammalian ortholog of Mel1c: evidence of rapid evolution in mammals. BMC Evol. Biol. *8*, 105.
45. Barrett, P., Ebling, F.J., Schuhler, S., Wilson, D., Ross, A.W., Warner, A., Jethwa, P., Boelen, A., Visser, T.J., Ozanne, D.M., et al. (2007). Hypothalamic thyroid hormone catabolism acts as a gatekeeper for the seasonal control of body weight and reproduction. Endocrinology *148*, 3608–3617.
46. Bechtold, D.A., Ivanov, T.R., and Luckman, S.M. (2009). Appetite-modifying actions of pro-neuromedin U-derived peptides. Am. J. Physiol. Endocrinol. Metab. *297*, E545–E551.
47. Li, J., Hand, L.E., Meng, Q.J., Loudon, A.S., and Bechtold, D.A. (2011). GPR50 interacts with TIP60 to modulate glucocorticoid receptor signalling. PLoS ONE *6*, e23725.